

This article was downloaded by:

On: 26 January 2011

Access details: *Access Details: Free Access*

Publisher *Taylor & Francis*

Informa Ltd Registered in England and Wales Registered Number: 1072954 Registered office: Mortimer House, 37-41 Mortimer Street, London W1T 3JH, UK



Liquid Crystals

Publication details, including instructions for authors and subscription information:

<http://www.informaworld.com/smpp/title~content=t713926090>

New ways to produce and measure low pre-tilt angles

J. T. Gleeson^a

^a Department of Physics and Astronomy, The University of Calgary, Calgary, AB, Canada

To cite this Article Gleeson, J. T.(1996) 'New ways to produce and measure low pre-tilt angles', *Liquid Crystals*, 20: 4, 453 – 458

To link to this Article: DOI: 10.1080/02678299608032059

URL: <http://dx.doi.org/10.1080/02678299608032059>

PLEASE SCROLL DOWN FOR ARTICLE

Full terms and conditions of use: <http://www.informaworld.com/terms-and-conditions-of-access.pdf>

This article may be used for research, teaching and private study purposes. Any substantial or systematic reproduction, re-distribution, re-selling, loan or sub-licensing, systematic supply or distribution in any form to anyone is expressly forbidden.

The publisher does not give any warranty express or implied or make any representation that the contents will be complete or accurate or up to date. The accuracy of any instructions, formulae and drug doses should be independently verified with primary sources. The publisher shall not be liable for any loss, actions, claims, proceedings, demand or costs or damages whatsoever or howsoever caused arising directly or indirectly in connection with or arising out of the use of this material.

New ways to produce and measure low pre-tilt angles

by J. T. GLEESON

Department of Physics and Astronomy, The University of Calgary,
Calgary, AB, T2N 1N4, Canada

(Received 11 September 1995; accepted 14 November 1995)

We report upon a new method for producing a homogeneous alignment with a low pre-tilt angle for nematic liquid crystals. This method is significantly simpler to implement than many existing methods, and requires knowledge of only the optical properties of the liquid crystal used. In addition, we have developed a new technique for measuring the pre-tilt angles that is straightforward as well as intuitively appealing. The sensitivity of this method increases as the pre-tilt angle decreases. Results obtained using this method agree satisfactorily with those yielded by traditional techniques.

1. Introduction

Producing homogeneous (planar) alignment of nematic liquid crystals with a low pre-tilt angle is a crucial step in almost every type of liquid crystal display. It also is often the critical difference in obtaining well-controlled, reproducible results in a programme of experiments studying liquid crystals. For these reasons, from the very beginning of the modern era of liquid crystal research, much attention has been paid to alignment technique [1]. One ubiquitous characteristic of homogeneous alignment is that the nematic director is rarely if ever exactly parallel to the aligning substrate, but tipped at a (usually small) angle θ_1 , the pre-tilt angle. Frequently this angle is not known, even though several ingenious methods have been devised to measure it [2]. Although effective, some of these methods can be either cumbersome to implement, requiring special configurations of apparatus, or can require detailed knowledge of the physical parameters of the liquid crystal. We report a new method of measuring the pre-tilt angle that not only requires no sophisticated apparatus but can actually be used with the standard set-up used for characterizing many types of liquid crystal displays. Moreover, this method requires only that one know the ordinary and extraordinary refractive indices of the liquid crystal.

2. Calculations

The main premise of our method of calculating θ_1 is that any non-zero pre-tilt will have a measurable effect on the onset of the splay Fréedericksz transition. This phenomenon is well known [3]; in this paper we examine it in detail and exploit it in order to measure the pre-tilt angle. Moreover, by looking only at onset the mathematics becomes considerably simpler. More importantly, we believe this analysis lends itself to a more intuitive understanding than do competing methods. We employ the

usual notation for the splay Fréedericksz transition, where the director remains in the x - z plane and the destabilizing field is in the \hat{z} direction. For zero pre-tilt, the undistorted configuration is $\hat{n} \parallel \hat{x}$. The distortion of the director is determined by its angle θ , with the x axis. We assume spatial uniformity in the x direction, so θ is a function only of z . The nematic is confined between two infinite planes, both normal to the z axis, and separated by a distance d . The pre-tilt angle specifies the boundary conditions, $\theta(z=0, d) = \pm \theta_1$.

It is important to look carefully at the director configuration in zero applied field. When $\theta_1 = 0$, we have the trivial solution $\theta(z) = 0$. For finite pre-tilt, there are two distinct cases. The first, and that most commonly found, is when the two substrates are arranged so θ_1 is the same on both surfaces. When one uses rubbing techniques, this is obtained by placing the substrates together so that the rubbing direction is anti-parallel on the two substrates. For this more important case, the zero-field, equilibrium director configuration is $\theta(z) = \theta_1$. We shall refer to this situation as *symmetric*. The second, where θ_1 has the opposite sign on opposing substrates, obtained by placing substrates together so that their rubbing directions are parallel, is less commonly used. For this case the zero-field, equilibrium director configuration $\theta(z) = \theta_1(1 - 2z/d)$. This is the *antisymmetric* situation; because it is less commonly encountered, it is discussed in detail in Appendix A. Both situations are depicted schematically in figure 1.

That part of the nematic's free energy, F , that depends on the director configuration can be expressed as an elastic term and an electric term [4]:

$$F = \frac{1}{2} \int_0^d \left[K_{11} \left(\frac{d\theta}{dz} \right)^2 - \frac{\Delta\epsilon V^2}{d^2} \sin^2 \theta \right] dz \quad (1)$$

where K_{11} is the splay elastic constant, $\Delta\epsilon$ is the anisotropy in the dielectric constants and V is the applied

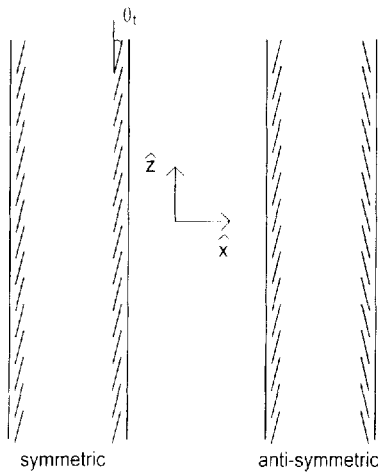


Figure 1. Schematic of the zero-field, equilibrium director configurations for the symmetric (left) and the antisymmetric (right) cases as described in the text.

potential difference. This expression ignores differences in the elastic constants and assumes that the electric field is independent of z . In Appendix B, we show that these assumptions have only negligible effects on the results; by making them we obviate the need for detailed knowledge of the elastic and dielectric constants of the liquid crystal. Our assumption of infinite anchoring strength will change the results somewhat, but the effect will be minimized because we are looking only at onset behaviour. After rescaling, this expression becomes

$$f = 2 \int_0^1 \left[\left(\frac{d\theta}{du} \right)^2 - \eta \sin^2 \theta \right] du, \quad (2)$$

where $f = 4Fd/K_{11}$, $u = z/d$, and $\eta = \Delta\epsilon V^2/K_{11}$. Again, since we are only interested in the onset we make the single mode *Ansatz* (for the symmetric case):

$$\theta(u) = \theta_t + A \sin(\pi u). \quad (3)$$

Substituting this into equation (2), expanding $\sin^2(\theta)$ to the fourth order in A then integrating yields,

$$f = 2\eta\theta_t^2 \left(\frac{\theta_t^2}{3} - 1 \right) + \frac{8\eta\theta_t}{\pi} \left(\frac{2\theta_t^2}{3} - 1 \right) A + (\pi^2 - \eta + 2\eta\theta_t^2) A^2 + \frac{32\eta\theta_t}{9\pi} A^3 + \frac{\eta}{4} A^4 \quad (4)$$

which we recognize as a Landau expansion in A . The equilibrium configuration is determined by choosing A such that $df/dA = 0$ and $d^2f/dA^2 > 0$. In figure 2 we plot the equilibrium value of A as a function of η for various values of θ_t . The reader will note that this behaviour is qualitatively very similar to a mean-field paramagnetic system near its Curie point, with θ_t playing the role of an external magnetic field.

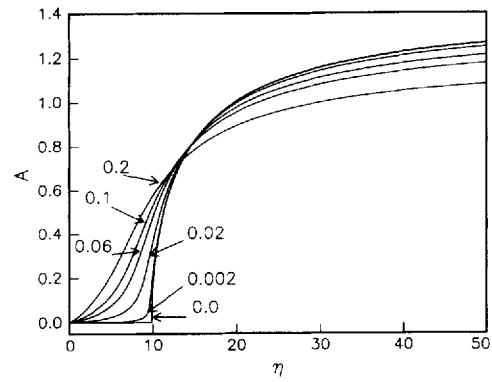


Figure 2. Equilibrium value of A versus η for various values of θ_t , as labelled on graph.

When $\theta_t = 0$, the transition from the undistorted state ($A = 0$) to a distorted state occurs at $\eta = \eta_c(0) = \pi^2$. This gives the well-known result for the critical voltage for the Fréedericksz transition, $V_c(\theta_t = 0) = E_c/d = \pi\sqrt{(\Delta\epsilon/K_{11})}$. When the pre-tilt angle is not zero, the Fréedericksz transition occurs at a lower voltage as was first pointed out by Rapini and Papoular [3]. We have plotted $\eta_c(\theta_t)$, the critical value of η , defined as that value where $dA/d\eta$ is maximum, as a function of θ_t in figure 3. We will see that the shift in critical voltage is an important factor in determining θ_t .

Our method of determining the pre-tilt angle is based on quantifying the degree to which the Fréedericksz transition, i.e. the ‘knee’ in the curves seen in figure 2, is rounded as the pre-tilt increases; a good measure of rounding is the slope of this curve at onset. If we can measure the slope at onset then we know θ_t . Figure 3 shows how this quantity decreases as the pre-tilt increases. This figure also demonstrates the increased sensitivity of this measurement for small pre-tilt angles. The problem now

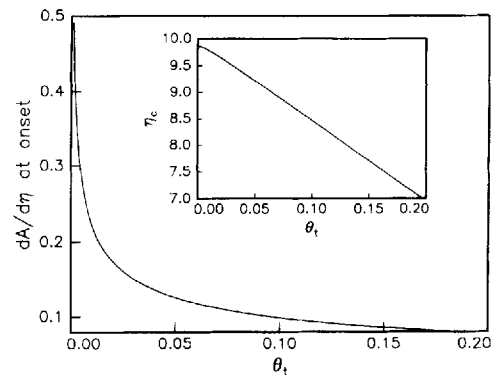


Figure 3. $dA/d\eta$ at onset as a function of pre-tilt angle. A is the equilibrium value that minimizes equation (4). Inset: critical value of η as a function of θ_t . η_c is that value where $dA/d\eta$ is maximum.

is that the quantity A , the director angle with \hat{x} midway between the plates, cannot be directly measured. We therefore must calculate how some measurable quantity will vary with both η and θ_1 , and compare that with experiment. We have chosen the optical phase difference between ordinary and extraordinary rays traversing the cell; the capacitance would work equally well. The optical phase difference δ is given by

$$\delta = \frac{2\pi}{\lambda} \int_0^d \left[\sqrt{(n_e^2 \sin^2 \theta + n_o^2 \cos^2 \theta)} - n_o \right] dz, \quad (5)$$

where n_e and n_o are, respectively, the extraordinary and ordinary refractive indices, and λ is the wavelength of light used. Therefore, for a given value of θ_1 and A , where A is chosen to minimize equation (4), and knowing n_e and n_o , we can perform the integration (numerically) and calculate δ . It is convenient to define a reduced phase difference $\delta_r \equiv \delta/\delta_0$, where δ_0 is the phase difference for the undistorted cell with zero pre-tilt; $\delta_0 = 2\pi(n_e - n_o)d/\lambda$. δ_0 will change very little for small values of θ_1 . In figure 4 we have plotted δ_r as a function of η for various values of θ_1 . In order to determine θ_1 , we plot the slope $d\delta_r/d\eta$ at onset as a function of θ_1 —see figure 5. We can then compare the expected value of this quantity with that obtained by experiment. Thus, by simply measuring the optical phase difference as a function of applied voltage as one induces the Fréedericksz transition, and using knowledge of the ordinary and extraordinary indices of refraction, the pre-tilt angle is immediately determined.

3. Experiments

We also present in this paper a description of a new and simple way to produce homogeneous alignment of nematic liquid crystals exhibiting low pre-tilt angle. We have found that a thin layer of the polymer poly(vinyl formal) (PVF), when deposited from solution and lightly rubbed in a single direction produces this effect. While rubbed polymer alignment layers are well known [1], PVF has significant advantages over other popular

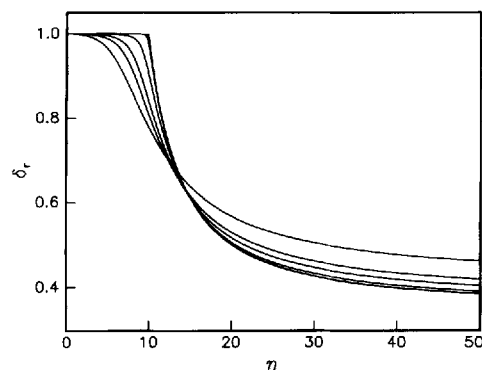


Figure 4. δ_r versus η for same values of θ_1 , as in figure 2.

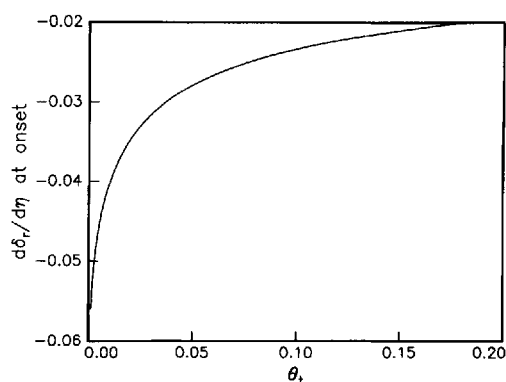


Figure 5. $d\delta_r/d\eta$ at onset as function of pre-tilt angle.

polymers that align. Firstly, PVF dissolves readily at room temperature in the carrier solvent (chloroform), unlike poly(vinyl alcohol) [1], or poly(ethylene terephthalate) [5]. Furthermore, the vapour pressure of chloroform is relatively high at room temperature eliminating the need to bake the solvent off. The concentration of PVF in solution is quite small compared to the concentration recommended for many common polymer solutions, and a comparatively short distance of rubbing is required.

PVF, as obtained from the manufacturer [6], is dissolved in chloroform to a concentration of ~ 0.05 wt %. Approximately 1–2 ml of this solution is dropped onto a spinning glass substrate. By the time the spin-coater has stopped, no trace of solvent remains. In fact, if the PVF concentration is too high (~ 0.5 wt %), an interesting ridge pattern characteristic of the solvent evaporating while spinning can be observed. Once coated, the substrate is rubbed unidirectionally with a cloth, and the two substrates are placed so that their individual rubbing directions are anti-parallel with spacers between them. The substrates are glued together and the liquid crystal introduced via capillary action. These operations are all performed in a laminar flow cabinet. We have obtained good quality alignment with different types of cloths, and currently use Super Polx 1200 wipers [7], which are specially knitted for clean-room application. The rubbing pressure is light, perhaps the weight of 20 g cm^{-2} . For the measurements we report, the sample cell is filled via capillary action with 4-*n*-pentylcyanobiphenyl (5CB) [8]. Sample cells are heated at least 10°C above the clearing point to eliminate flow alignment effects. We have obtained good quality homogeneous alignment (as confirmed by polarized light microscopy) using PVF with every nematic substance we have to date tried.

As described above, we wish to know the optical phase difference as a function of applied potential difference in the \hat{z} direction. We use glass substrates having a transparent indium–tin oxide coating to apply the potential

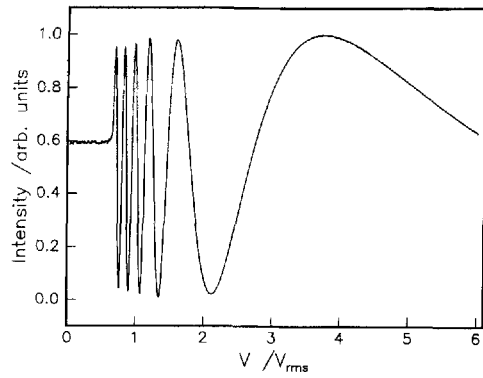


Figure 6. Intensity of light transmitted through the sample cell with polarizers crossed at $\pm 45^\circ$ to the rubbing direction on either side as a function of voltage applied to the cell.

difference. A function generator provides a 1 kHz sinusoidal signal of variable amplitude, and a $2 \mu\text{F}$ capacitor in series eliminates the possibility of d.c. offset. The sample is placed between polarizer and analyser crossed with their axes at $\pm 45^\circ$ to the rubbing direction on the substrates. A frequency stabilized He-Ne laser is shone through this stack, and the transmitted intensity is monitored by a photodiode. As the Fréedericksz transition occurs, the transmitted intensity varies as $I \propto \sin^2(\delta/2)$. See figures 6 and 7 for an example of optical phase difference data, and the intensity data from which it was derived.

The only thing that remains to be done is to find the slope at onset of a curve such as in figure 6, and compare it to figure 5. There is however one subtlety. Recall that η is defined as $\pi^2(V/V_c(0))^2$, where $V_c(0)$ is the critical voltage for the case $\theta_t = 0$, and that V_c can change appreciably with θ_t ; cf. figure 3. To account for this, we normalize V by the observed value of the critical field

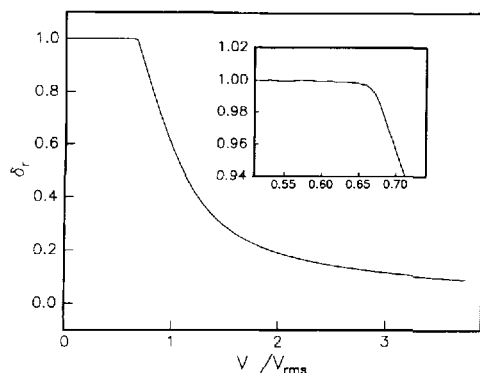


Figure 7. Reduced optical phase difference between ordinary and extraordinary rays, δ_r , as a function of voltage applied to the cell. Inset: magnification of the Fréedericksz transition region.

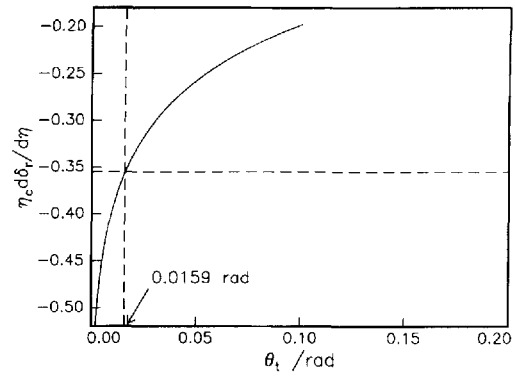


Figure 8. Example of how θ_t is obtained from the slope of δ_r at onset and $\eta_c \cdot d\delta_r/d\eta$ is computed, and multiplied by η_c . A horizontal line is located at the experimentally determined value of the slope of δ_r as a function of $(V/V_c)^2$; θ_t is the abscissa where these curves cross. In this example, we have determined the pre-tilt angle to be 0.91° .

$V_c(\theta_t)$. We then find the minimum value of the slope of δ_r with respect to the square of this reduced quantity. We multiply the ordinates of the two curves in figure 3 (inset) and figure 5 together. One looks for the abscissae on this new curve where the ordinate has the value of slope at onset obtained from experiment. That yields θ_t . See figure 8 for an example. In figure 9 we plot the pre-tilt angle obtained using this method versus the temperature, for the PVF alignment method outlined earlier. We used the values of Dunmur *et al.* [9] for the indices of refraction. For most of the nematic range, we see that PVF when used in this way with 5CB yields a pre-tilt angle that is less than 1° . Figure 10 shows a crystal rotation curve [2] of a PVF aligned sample for comparison. Using this traditional method, we have measured the pre-tilt to be 1.2° , in excellent agreement with the new method reported here.

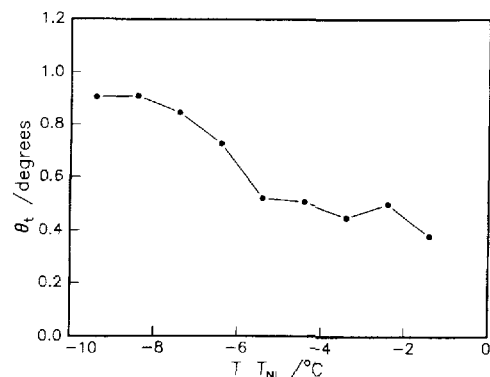


Figure 9. Pre-tilt angle θ_t as a function of temperature for 5CB aligned homogeneously by poly(vinyl formal) as determined by the Landau expansion method detailed in the text.

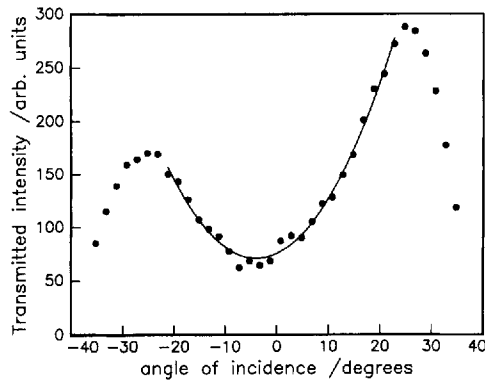


Figure 10. Crystal rotation curve for a 50 μm sample of 5CB aligned with rubbed PVF in the manner described in the text. Using published values for the indices of refraction we find the pre-tilt angle to be 1.2° .

4. Conclusions

We have demonstrated a new and easy to implement method of producing homogeneous alignment of nematic liquid crystals with a low pre-tilt angle. This method is not only convenient for many applications in liquid crystal research where such alignment is required, but should also be practical for those types of liquid crystal displays, for example, twisted nematic, where alignment layers are of paramount importance in determining the quality of the device.

We have also developed a novel, and in our opinion, intuitively appealing technique to measure the pre-tilt angle, based on the common observation that the Fréedericksz transition becomes more rounded as the pre-tilt angle increases. No special equipment or configurations are needed beyond what is commonly employed in routine characterization and analysis of sandwich-type liquid crystals displays, and only the optical properties of the liquid crystal used need be known.

Appendix A: Antisymmetric alignment

To prevent the formation of tilt domains (walls) in the Fréedericksz transition, sample cells are commonly constructed so that the rubbing directions on the substrates are anti-parallel. This arrangement gives the same sign pre-tilt angle on both boundaries, so that one preferred sign of the director tilt occurs at the Fréedericksz transition. If the substrates are assembled so that the rubbing directions are *parallel*, this will promote the occurrence of tilt domains. However, considering this case does lead to some interesting results. As we saw previously, the undistorted director configuration for this case is $\theta(z) = \theta_t(1 - 2z/d)$. Making the same single mode *Ansatz* as before, $\theta(z) = \theta_t(1 - 2z/d) + A \sin(\pi z/d)$, and inserting

this into the free energy F and integrating, still keeping terms up to fourth order in A yields

$$f = \left(8 - \frac{2\eta}{3} + \frac{2\eta\theta_t^2}{15}\right)\theta_t^2 + \left(\pi^2 - \eta + \frac{2\eta\theta_t^2}{3} - \frac{4\eta\theta_t^2}{\pi^2}\right)A^2 + \frac{\eta}{4}A^4. \quad (\text{A } 1)$$

This is obviously very different from the anti-parallel case considered earlier, but identical in form to the case $\theta_t = 0$. The coefficients are different, but with only even powers of A , the Fréedericksz transition occurs where the coefficient of the quadratic term vanishes. Furthermore, the transition should be perfectly sharp, but now

$$\eta_c^{(\text{AS})}(\theta_t) = \frac{\eta_c(0)}{\left(1 - \left(\frac{2}{3} - \frac{4}{\pi^2}\right)\theta_t^2\right)} = \frac{\eta_c(0)}{1 - 0.261382\theta_t^2}. \quad (\text{A } 2)$$

So this configuration should not only give a Fréedericksz transition with no rounding, but should actually have a higher threshold voltage than the zero pre-tilt case.

Appendix B: Elastic constant anisotropy and inhomogeneous electric field

When $K_{11} \neq K_{33}$, and when the electric field is not assumed to be independent of z , equation (1) becomes

$$F = \frac{1}{2} \int_0^d (K_{11} \cos^2 \theta + K_{33} \sin^2 \theta) \left(\frac{d\theta}{dz}\right)^2 dz - \frac{1}{2} V^2 \left[\int_0^d \frac{dz}{\epsilon_1 \cos^2 \theta + \epsilon_\perp \sin^2 \theta} \right]^{-1}.$$

We shall refer to this as the *comprehensive* case, in contrast to the simple case discussed previously. Making the same *Ansatz* and expansion to fourth order in A as before, the new coefficients in the Landau expansion (equation (4)) are

$$\begin{aligned} c_0 &= 2\eta\theta_t^2 \left(\frac{\theta_t^2}{3} - 1\right) - \frac{2\eta}{\gamma}, \\ c_1 &= \frac{8\eta\theta_t}{\pi} \left(\frac{2\theta_t^2}{3} - 1\right), \\ c_2 &= \left(-\frac{16\eta\gamma}{3} - 4\eta\gamma^2 - \frac{\kappa\pi^2}{3} + \frac{32\eta\gamma^2}{\pi^2} + \frac{128\eta\gamma}{3\pi^2}\right)\theta_t^4 \\ &\quad + \left(\kappa\pi^2 + 4\eta\gamma - \frac{32\eta\gamma}{\pi^2} + 2\eta\right)\theta_t^2 - \eta + \pi^2, \\ c_3 &= \left(-\frac{16\kappa\pi}{9} - \frac{64\eta\gamma}{9\pi} - \frac{128\eta\gamma^2}{\pi^3} + \frac{8\eta\gamma^2}{\pi}\right)\theta_t^3 \\ &\quad + \left(\frac{8\kappa\pi}{3} + \frac{32\eta}{9\pi} + \frac{8\eta\gamma}{3\pi}\right)\theta_t, \end{aligned}$$

$$c_4 = \left(-\frac{160\eta\gamma^3}{3\pi^2} - \frac{512ne}{27\pi^2} + \frac{87\eta\gamma^2}{4} - \frac{1376\eta\gamma^2}{9\pi^2} \right. \\ \left. + \frac{11\eta\gamma}{3} + \frac{57\eta\gamma^3}{4} - \frac{512\eta\gamma^3}{\pi^4} \right) \theta_t^4 \\ + \left(-\frac{\kappa\pi^2}{2} + \frac{112\eta\gamma^2}{3\pi^2} - 5\eta\gamma + \frac{256\eta\gamma}{9\pi^2} - \frac{21\eta\gamma^2}{4} \right) \theta_t^2 \\ + \frac{\kappa\pi^2}{4} + \frac{\eta}{4} + \frac{\eta\gamma}{4}$$

where c_n is the coefficient of $A^n\kappa = K_{33}/K_{11} - 1$, and $\gamma = \Delta\varepsilon/\varepsilon_{\perp}$. The critical voltage for the Fréedericksz transition when $\theta_t = 0$ is not changed by either non-zero κ or the extra electric field terms. As can be easily seen by considering the zero pre-tilt situation, one large effect of including the refinements above is to substantially decrease the predicted saturation value A_{∞} , defined to be $\lim_{n \rightarrow \infty} A(\eta)$. This is no surprise because Landau theory is only valid for small A , as at onset. However, this saturation value does scale $dA/d\eta$, even at onset. To compensate for this, once $A(\eta)$ is calculated, we can divide it by the calculated value of A_{∞} . In figure 11 we show the effect of including these corrections, using published values of κ [10] and γ [9], on $dA/d\eta$ at onset divided by A_{∞} ; nowhere is the correction larger than 20 per cent. Because δ_r is what we measure, we must also compensate for A_{∞} in this quantity. As before, after $A(\eta)$ is calculated, we divide it by A_{∞} ; we then must then rescale it by $\sqrt{2 - \theta_t}$, which is A_{∞} for the simpler case, so that we can directly compare to the comprehensive case. We then used the rescaled A to find δ_r , via equation (5). Clearly the simpler calculation discussed previously works so well because there (when the pre-tilt angle is zero) $A_{\infty} = \sqrt{2}$, very close to $\pi/2$. In figure 12 we plot the calculated values for $d\delta_r/d\eta$ at onset as a function of θ_t ,

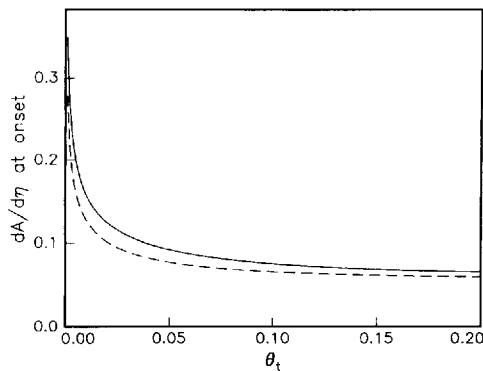


Figure 11. $dA/d\eta$ at onset for the comprehensive case (dashed) as compared to the simpler case (solid). $A(\eta)$ for the comprehensive case has been rescaled to have the same value of A_{∞} . The differences between these two curves nowhere exceed 20 per cent.

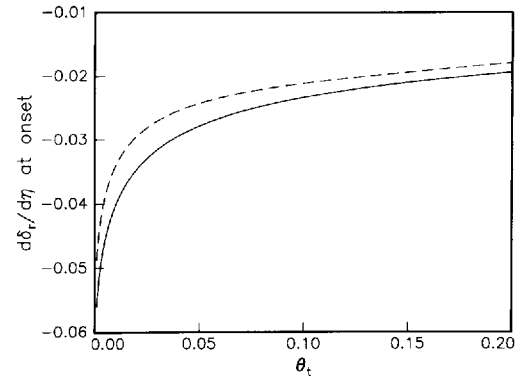


Figure 12. $d\delta_r/d\eta$ at onset for the comprehensive case (dashed) as compared to the simpler case (solid). For the comprehensive case, the values of $A(\eta)$ from which δ_r is obtained have been rescaled to have the same value of A_{∞} . The differences between these two curves nowhere exceed 20 per cent.

after rescaling A_{∞} , comparing the simpler calculation discussed previously and this more comprehensive one. Again, the differences are not significant.

This insensitivity to such corrections is of course a consequence of choosing a method that looks only at the behaviour at onset. There are two important benefits of making the assumption that these corrections are negligible. Firstly, and arguably the more important, is that the whole phenomenon is vastly simpler and hence more intuitively understandable, and secondly one does not need to know either the elastic or the dielectric constants of the liquid crystal employed.

The numerical integration routine used was written by P. Palfy-Muhoray. This work was supported by the Natural Sciences and Engineering Research Council and the University of Calgary.

References

- [1] COGNARD, J., 1982, *Mol. Cryst. liq. Cryst., Supp. 1*.
- [2] SCHEFFER, T. J., and NEHRING, J., 1987, *J. appl. Phys.*, **48**, 1783.
- [3] RAPINI, A., and PAPOULAR, M., 1969, *J. Phys. (Colloq.)*, **30**, C4-54.
- [4] One could equivalently consider a magnetic field by replacing the second term with $-\Delta\chi H^2 \sin^2(\theta)$.
- [5] GEARY, J. M., GOODBY, J. W., KMETZ, A. R., and PATEL, J. S., 1987, *J. appl. Phys.*, **62**, 4100.
- [6] Aldrich Chemicals Inc.
- [7] Berkshire Corp., Great Barrington, MA, U.S.A.
- [8] BDH Chemicals, Ltd., Poole, England.
- [9] DUNMUR, D. A., MANTERFIELD, M. R., MILLER, W. H., and DUNLEAVY, J. K., 1978, *Mol. Cryst. liq. Cryst.*, **45**, 127.
- [10] BUNNING, J. D., FABER, T. E., and SHERRELL, P. L., 1981, *J. Phys. (Paris)*, **42**, 1175.